

*High Explosives Skid
Impact Initiation Study*

*Armando S. Vigil
James M. Bunch
Dwight L. Jaeger
Paul D. Smith
Ernest E. Abeyta*



DISCLAIMER

This report was prepared as an account of work sponsored by an agency of the United States Government. Neither the United States Government nor any agency thereof, nor any of their employees, makes any warranty, express or implied, or assumes any legal liability or responsibility for the accuracy, completeness, or usefulness of any information, apparatus, product, or process disclosed, or represents that its use would not infringe privately owned rights. Reference herein to any specific commercial product, process, or service by trade name, trademark, manufacturer, or otherwise does not necessarily constitute or imply its endorsement, recommendation, or favoring by the United States Government or any agency thereof. The views and opinions of authors expressed herein do not necessarily state or reflect those of the United States Government or any agency thereof.

MASTER

THIS IS A COPY OF THE DOCUMENT IS UNCLASSIFIED

212

CONTENTS

	ABSTRACT	1
I.	INTRODUCTION	1
II.	APPROACH	2
III.	EXPERIMENTAL RESULTS	3
	A. Go/No-Go Detonation Criteria	3
	B. Air Gun Data	4
	C. Drop Tower Data	7
	D. Infrared Detectors	10
IV.	COMPUTER MODELS AND SIMULATIONS	10
	A. EXPLO Thermal Analysis	11
	B. DYNA3D Stress Analysis	12
	C. ABAQUS Heat Transfer and Stress Analysis	20
V.	SUMMARY AND CONCLUSIONS	20
	REFERENCES	22

LIST OF FIGURES

1	Schematic diagram of the HE skid impact initiation experiment.	3
2	Impact velocity and corresponding drop height capability of the 155-mm air gun.	5
3	Original and modified projectile assembly designs.	6
4	Schematic diagram of vertical drop test configuration.	8
5	Finite element mesh of the projectile assembly as it impacts an inclined aluminum plate.	13
6	Deformation and maximum principal strain of 1-inch diameter sample impacting a target plate inclined 45 degrees.	16
7	Deformation and maximum principal strain of 10-inch diameter sample impacting a target plate inclined 45 degrees.	17
8	Deformation and maximum principal strain of 1-inch diameter sample impacting a target plate inclined 30 degrees.	18
9	Deformation and maximum principal strain of 3-inch diameter sample attached to a modified projectile impacting a target plate inclined 30 degrees.	19

LIST OF TABLES

1	PBX 9404 HE Skid Impact Ignition Data	9
2	Material Properties used in DYNA3D Skid Impact Analysis	14

HIGH EXPLOSIVES SKID IMPACT INITIATION STUDY

by

Armando S. Vigil, James M. Bunch, Dwight L. Jaeger,
Paul D. Smith, and Ernest E. Abeyta

ABSTRACT

The objective of this study was to develop a better quantitative understanding of explosive behavior under skid impact conditions. We evaluated the effects of sample weight, impact velocity, contact surface area at impact, target surface roughness, and target material on the skid impact HE ignition threshold. We also quantified the effects of two parameters that had never been fully investigated in the standard skid impact sensitivity test: explosive sample size and angle of incidence. These parameters were studied experimentally by conducting a series of tests, and analytically, with a number of one-, two-, and three-dimensional computer models. This study is the first phase in a program to measure the transient heat produced in the ignition of a high explosive sample as it impacts an infrared (IR) transmissive target. We will use the experimentally derived data to enhance our ability to predict the onset of ignition in impact-heated high explosives.

I. INTRODUCTION

The ignition of high explosives under skid impact conditions has never been satisfactorily understood. It is not entirely predictable. The results of our initial tests and structural analyses on this project indicate that a small-diameter secondary high explosive hemisphere may ignite more readily at lower impact velocities than at high ones. At lower velocities the sample holds together long enough for heat from combined compression, friction, and shearing forces to build to ignition. This is an important safety issue. Safety is the principal

motivation behind the work done in this project. Furthermore, a better understanding of the mechanism may affect the design of some weapons in extreme environments, such as artillery-fired projectiles and earth penetrators.

Von Holle, LLNL, has demonstrated the feasibility of the measurement of the infrared emission of radiation from shocked explosives using infrared equipment.¹ He observed chemical hot spots that are postulated as nucleation sites for buildup to detonation. However, while we are interested in investigating the threshold of ignition, Von Holle confines his work to shock heating at very high pressures. His pressures are produced by normal impact velocities twenty times that of our drop tower or projectile launcher capability. Dyer and Taylor, AWRE, and Randolph, Hatler, and Popolato, LANL, have investigated the friction-heating mechanism in secondary high explosives at their ignition thresholds.^{2,3} They investigated the effects of explosive weight, drop height, target thermal conductivity, and surface roughness on HE initiation. We intend to probe further into the heat buildup mechanism that determines the go/no-go ignition threshold. We postulate that it occurs in the thin region of impact-heated high explosive at the HE-target interface. We plan to use our infrared equipment to investigate what occurs in this region.

II. APPROACH

In the standard skid tests,⁴ a bare explosive charge hits a rigid surface at an oblique angle. This simulates the condition where a bare charge is accidentally dropped. These tests have only been done with large samples, between 9 and 132 kg in weight, at incident angles of 14 and 45 degrees. The variables are drop height, angle of impact between target and explosive, and target surface conductivity and roughness. We quantify these variables as well as the effect of small sample size in the work described here.

Our approach in this program will be to impact small high explosive charges onto infrared-transmissive targets and measure the temperature at the HE-target interface. We use two methods to achieve impact: a 155-mm diameter projectile launcher powered by compressed air, and a 46-meter drop tower. Both facilities are located at K-Site (TA-11). A schematic diagram of the HE impact initiation experiments is shown in Fig. 1. The high explosive sample impacts the window, either salt (NaCl) or sapphire, at an oblique incident angle. Two InSb infrared detectors with selected band-pass filters will be used

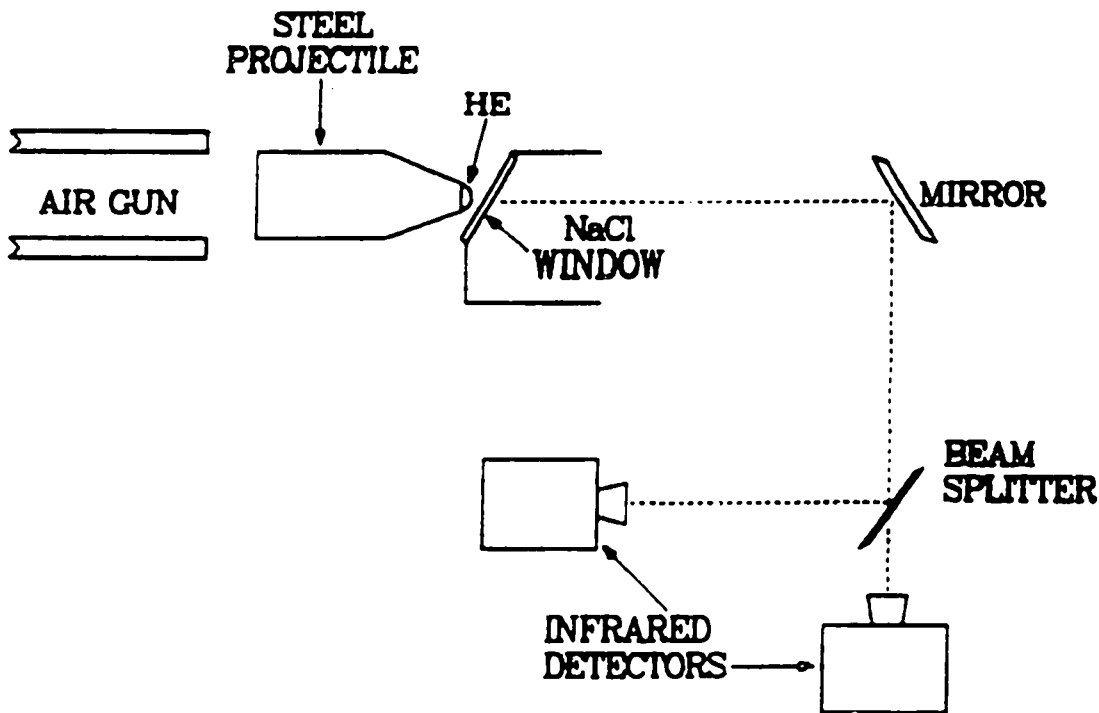


Fig. 1. Schematic diagram of the HE skid impact initiation experiment.

to record the impact-induced temperature rise through the window using an appropriate mirror/beam splitter configuration. If the air gun is used, the projectile assembly is deflected into a catch tank after bouncing off the target. The signals from both detectors will be processed to obtain a transient temperature response curve.

III. EXPERIMENTAL RESULTS

A. Go/No-Go Detonation Criteria

We established a go/no-go detonation criteria by measuring the overpressures produced from 1-inch diameter hemispheres of PBX 9501 high explosive. PBX 9501 is a plastic-bonded secondary explosive composed of 95 wt% HMX, 2.5 wt% Estane, and 2.5 wt% BDNPA/BDNPF. We ignited the hemispheres using exploding bridge wire (EB-1) detonators cemented to the flat face of each 9-gram charge. The pressure gauges used were Endevco 8510B piezoresistive transducers mounted to 4-inch square aluminum plates. We measured average peak reflected pressures of 1269 and 6.9 psi for the gauges located 11 and 42 inches from the HE, respectively. No pressure was recorded on any of the gauges when projectiles without HE were fired from the air gun onto a target

plate. We can readily distinguish between the overpressure from the detonation of 9 grams of HE at the target surface and the air gun's muzzle blast. We do not plan to test HE samples smaller than 9 grams.

B. Air Gun Data

Our air gun projectile assembly consists of a 1-inch diameter hemisphere sample glued to a 4-inch high cone of 900-10 inert HE, attached to a 4-inch long, 155-mm diameter steel cylinder. The mass of the projectile assembly, 11 kg, approximates the mass of the standard LLNL-Pantex skid sensitivity test specimen.⁵ The air gun is enabled for firing by inserting the projectile assembly into the gun through the breech end and installing the breech closure. The projectile acts as a valve and seals off the open end of a 6-inch diameter high pressure hose. When the end of this hose is sealed, a large tank, attached to the other end, may be pressurized with an air compressor. The projectile is launched remotely by using a solenoid valve to inject a burst of air between it and the closed end of the gun. This pushes the projectile past the hose opening and allows the high pressure air to rush in and eject the projectile. It travels about three feet horizontally before it impacts the target.

We have successfully propelled 11-kg projectiles to muzzle velocities ranging from 5 to 35 m/s. We measure the projectile velocity using magnetic proximity switches mounted on the muzzle end of the air gun, the Spin Physics 2000 High Speed Video System, and high-speed photography. The projectile velocity has been correlated to tank air pressure and equivalent drop height, a standard measure of comparing the relative safety of high explosives. The data obtained using these three velocity measuring systems is shown in Fig. 2. We have exceeded the maximum velocity attainable on the 46-meter drop tower and can go to higher pressures/velocities if necessary. A catch tank for the projectile was fabricated, installed, and tested. The catch tank allows us to retrieve and reuse the undamaged projectile components with a minimum of reconditioning.

The air pressure versus projectile velocity data shown in Fig. 2 was obtained using 1-inch diameter wax or explosive simulant hemispheres. Our initial tests using live HE were done using PBX 9404 samples. PBX 9404 HE is a plastic-bonded secondary explosive composed of 94 wt% HMX, 3 wt% nitrocellulose, 3 wt% CEF, and 0.1 wt% DPA. We used PBX 9404 instead of PBX 9501 HE samples because the 50% drop height of PBX 9404 is one-sixth that of

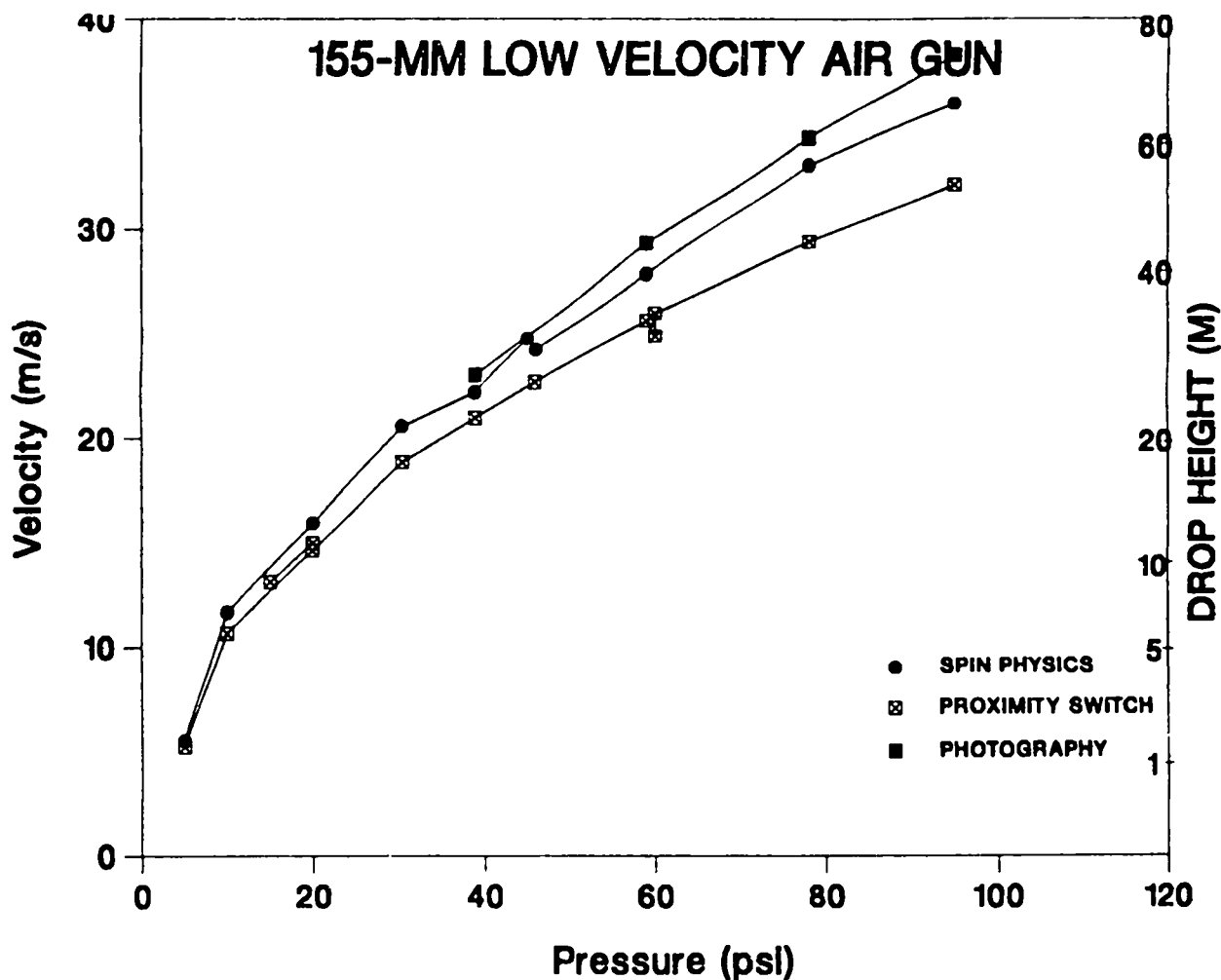


Fig. 2. Impact velocity and corresponding drop height capability of the 155-mm air gun.

PBX 9501 HE. The 50% drop height is the estimated median height, where the probability for an event is one-half.⁶ The samples were fired onto salt windows bonded to 1/4-inch thick plywood boards. The boards were bolted to a large steel shot stand at a 45 degree angle to the initial projectile direction. Because we were not able to obtain ignition with the salt/plywood target, we replaced the plywood board with a sturdier target support made of 3/8-inch thick aluminum plate. We used epoxy adhesive to bond sheets of 80-grit garnet paper (sandpaper) to 4 x 11 inch plates of aluminum bolted to the shot stand. The 50% drop height of a 10-inch diameter hemisphere of PBX 9404 HE on a sandpaper target at a 45 degree incident angle is 4 feet.⁴ Surprisingly, we did not obtain ignition of any of the 1-inch diameter samples, even when impacting PBX 9404 HE on sandpaper at a velocity that corresponds to a drop height of 115 feet. In an effort to obtain ignition we also fired 1-inch diameter hemispheres of PBX 9404 and PBX 9501 HE at glass, salt, and fused-quartz targets bonded to 3/8-inch aluminum plate at velocities that correspond to drop heights ranging from 17 to 67 feet. There was no evidence of ignition in any of these shots.

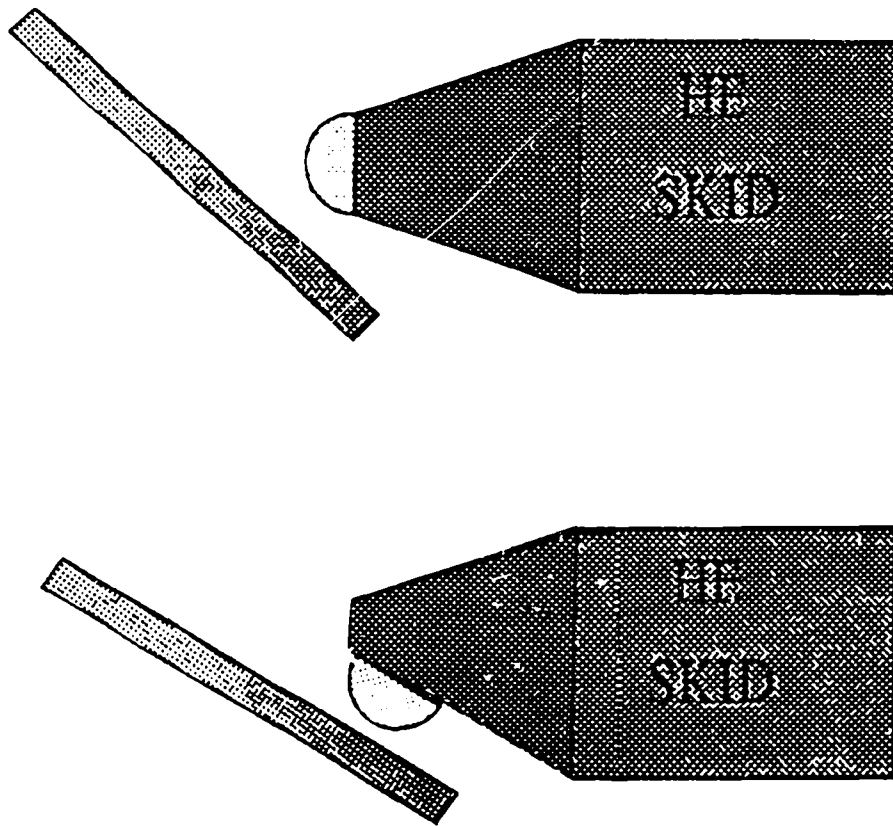


Fig. 3. Original and modified projectile assembly designs.

Dyer and Taylor determined that it takes about 0.5 ms for heat from friction, compression, and shear mechanisms at the impact interface to build to ignition.² Our initial three-dimensional structural analyses of the impact event indicate that a 1-inch diameter explosive hemisphere breaks apart 0.2 to 0.5 ms after impacting a target plate inclined 45 degrees to the angle of incidence. Our analyses reveal that impacting a plate set at a 30 degree angle of incidence allows more time for heat buildup. However, the analyses also revealed that when the target plate is inclined 30 degrees or less to the initial projectile direction, the forward end of the inert support cone strikes the target early enough that it interferes with the impact of the sample hemisphere. We eliminated this interference by modifying the design of the projectile assembly. We machined a flat surface on the side of the inert cone and bonded the 1-inch diameter hemispheres to this surface. The modified projectile assembly, used in the shallow incident angle tests, is shown in Fig. 3 along with the original projectile assembly design.

To determine if this new test configuration would perform as expected, we fired two shots with 1-inch diameter wax hemispheres bonded to the modified inert cones. The sandpaper-covered aluminum target plate was attached to the shot stand at a 30 degree angle of incidence. We measured projectile velocities corresponding to drop heights of 18 and 38 feet. There was a 2-inch long

wax smear on each sandpaper target after the tests. From the location of the smear we feel that we can hit our target accurately because there is little or no rotation of the projectile when it exits the gun.

We fired the projectile with a 1-inch diameter PBX 9404 explosive hemisphere bonded to the flat surface of the inert cone into a sandpaper covered aluminum target plate set at a 30 degree incident angle. The impact velocity was 8.5 m/s, corresponding to a drop height of 12.1 feet. We did not obtain ignition or any measurable overpressure. Because of cost and schedule constraints, we have not conducted tests at higher impact velocities.

We performed a spectroscopic analysis of the HE smear on the plate and found no evidence that the PBX 9404 HE had been heated past the beta-to-delta solid-to-solid phase transition temperature of 190°C. However, we found hydrocarbon-based oil contamination on the target. The oil may have come with the compressed air released from the gun muzzle. It may affect heat transfer or provide heat sink effects at the HE/sandpaper interface and hinder HE ignition. Dyer and Taylor report that initiation normally observed on a dry surface does not occur when water is present.² We need to eliminate all oil contaminants in our air gun shots if we hope to obtain relevant skid impact HE ignition data.

C. Drop Tower Data

We cannot test explosives larger than a few grams at the air gun facility because of the proximity of support equipment and structures. The K-Site drop tower facility allows us to drop large, 10-inch diameter high explosive charges from a height of up to 46 meters. Most skid sensitivity data published in the literature were obtained using this and similar drop towers.^{4,5} The data are obtained by allowing an uncased hemispherical charge to drop from the tower onto a rigid target at an oblique angle. A schematic of the vertical drop test configuration is shown in Fig. 4. Results reported are the drop height that produces events in 50% of the trials and the average overpressure. In another version of the test, the hemispherical charge is allowed to swing down in a harness on the end of a cable and strike a rigid horizontal target at a predetermined angle. This version was not used for the work described in this report. We used the vertical drop test to determine the 50% drop height of progressively smaller explosive samples when we were not able to obtain

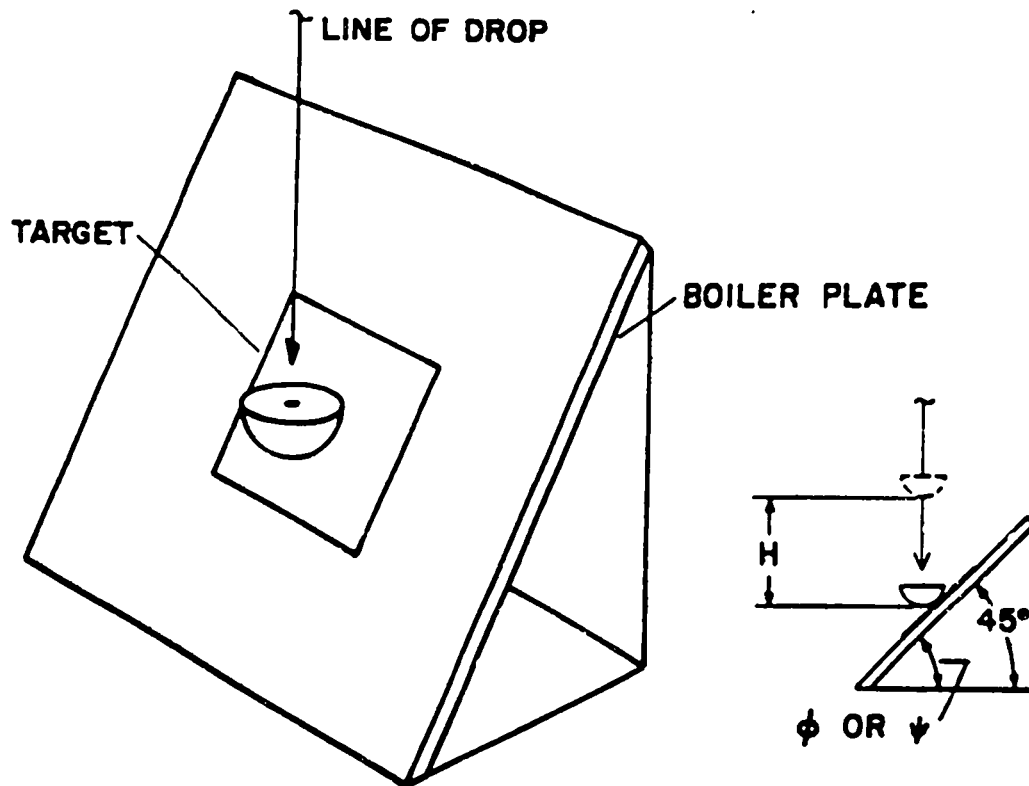


Fig. 4. Schematic diagram of vertical drop test configuration.

ignition of 1-inch diameter PBX 9404 HE hemispheres using the air gun.

In this test series, 6-, 3-, and 1-inch diameter samples were dropped. The 6- and 3-inch diameter explosive samples are bonded to 1/2- and 3/8-inch thick Micarta disks, respectively. The disks were drilled and tapped at the center to hold a lanyard by which the specimens were suspended from the drop release mechanism. Because of their small size, we mounted the 1-inch diameter samples on either HE simulant cones or 1-inch diameter wood dowels. We used guide cables for the 1-inch diameter drops. The guide cables ensure accuracy in hitting the target and greatly restrict rotation of the specimens upon impact. In all cases the targets are 80-grit garnet paper bonded with epoxy adhesive to 1/4-inch thick aluminum plates. The target plates are supported on a 5 foot square by 4.5-inch thick steel target stand inclined 45 degrees to the vertical.

The 50% drop height for the standard 10-inch diameter hemispheres of PBX 9404 HE, determined from tests conducted several years ago, is 4 feet. Assuming a lognormal distribution for the go/no-go events, the 50% drop height of the 6-inch specimens is 5.3 feet.⁶ Impact spot diameters on the charges and targets were from 5/8 to 3/4 inch for the no-goes that remained intact. Not

Table 1. PBX 9404 HE Skid Impact Ignition Data

Test Config.	Total Mass(kg)	Charge Dia.(in.)	Incident Angle(deg)	50% Drop Height(ft)	Max.Height Tested(ft)	Minimum EXPLO Ign. Height(ft)
Vert.Drop	8.7	10	45	4.0	15	1.8
Vert.Drop	2.0	6	45	5.3	6.3	5.2
Vert.Drop	0.3	3	45	23.7	50	19.8
Vert.Drop	0.6	1	45	-	15	8 ^a
Air gun	11	1	45	-	115	-
Air gun	11	1	30	-	12.1	-

^aThis drop height was calculated using the additional 600 g weight of the inert cone that was attached to the sample.

all the reactions were high-order detonations. The 50% drop height of the 3-inch diameter PBX 9404 HE samples is 23.7 feet. We measured impact spot diameters from 3/8 to 1/2 inch for the no-goes that remained intact in this series. Most of the reactions were low-order partial detonations. The 1-inch diameter HE samples did not ignite at drop heights up to 15 feet, despite the guide cables and the additional weight of the inert cones or wood dowels attached to them. We have not been able to test at higher drop heights. Remember that we were not able to detonate 1-inch diameter PBX 9404 HE hemispheres using the air gun at an equivalent drop height of 115 feet. As before, in the events where no reaction occurred, we conducted a spectroscopic search of the sandpaper targets for beta-to-delta phase change in the HMX crystals of the PBX 9404 HE. We found no evidence that the 1-inch diameter samples had been heated past the phase change temperature of 190°C.

A summary of the air gun and drop test data is given in Table I. Note that the 50% drop height of the 1-inch diameter hemispheres has not been determined. To accomplish the remaining objectives of this program, we must determine the minimum HE sample size that can be consistently initiated through skid impact. Because of the difficulty in igniting the 1-inch hemispheres, we will drop either 3-inch diameter hemispheres from the tower or use the air gun to fire 1/2-inch high x 3-inch diameter spherical segments onto infrared-transmissive targets.

D. Infrared Detectors

Our HE skid impact initiation program requires that we use suitable temperature measuring devices. We ran a model parameter study to optimize the detector wavelength bands for a two-color infrared pyrometer for use in the temperature range 150 to 300°C. We evaluated the suitability of various detectors for use in the selected wavelength range, given the expected target parameters. We determined that liquid nitrogen cooled InSb or gold-doped Ge should give usable signal-to-noise ratios for the proposed experiments. We tested a borrowed gold-doped Ge detector on a simulated target in an oven. It gave an easily detectable signal at 150°C. Because InSb is supposed to give a factor of ten better sensitivity than gold-doped Ge, we purchased a pair of InSb detectors mounted on Dewars with appropriate band-pass filters. We installed them in camera mounts with provisions for aiming and alignment through BaF lenses. We designed and built a system to calibrate the detectors by producing pulsed thermal signals using an oven with a shuttered opening.

We calibrated the InSb pyrometer by measuring the ratio of the responses of the two detectors aimed at a source heated to various temperatures in the range of interest. Using various simulated targets, we evaluated the pyrometer's sensitivity and temperature resolution in measuring the temperature of a simulated "hot spot" surrounded by a region of lower temperature. We should be able to obtain transient temperature response measurements from the sample/window interface. By comparing the response measurements of inert and reactive material, we hope to learn more about the melt phase that we postulate to occur in the skid impact ignition of high explosives.

IV. COMPUTER MODELS AND SIMULATIONS

Three computer codes were used in our modeling effort. They are EXPLO, DYNA3D, and ABAQUS. The EXPLO thermal analysis code,⁷ which includes a subroutine that models the skid impact of explosives on different target slabs, allows us to predict HE ignition. The DYNA3D code⁸ allows nonlinear dynamic analyses of structures in three dimensions. The ABAQUS code⁹ allows fully coupled temperature-displacement analyses to predict material deformation and HE ignition.

A. EXPLO Thermal Analysis

EXPLO was written by D. L. Jaeger and A. S. Vigil. It uses the finite difference method to calculate temperature fields and times to initiation for explosive materials.⁷ The code is one-dimensional and is programmed for cartesian, cylindrical, and spherical coordinates. Temperature-dependent properties, phase changes, and multiple heat source terms use Nth-order Arrhenius kinetics for each material component. To predict the initiation of high explosives caused by skid impact, EXPLO contains a subroutine that computes the energy generated by a sliding surface as a function of several variables and time. These variables are drop height, weight, shear strength, and skid angle. EXPLO uses Randolph et al.'s definition of heat flux generated at the sliding surface between the HE and the target slab.³ The flux is calculated as

$$q = \mu\sigma V/J, \quad (1)$$

where μ is the apparent coefficient of friction (equal to the ratio of tangential to normal contact forces), σ is the normal contact pressure (in this case equal to the plastic flow stress of the explosive), V is the sliding velocity, and J is the conversion factor from mechanical to thermal units.

We used the EXPLO code to determine the minimum drop height to ignition for different weights of PBX 9404 HE dropped on an aluminum plate covered with sandpaper. The weights correspond to different diameter hemispheric test samples. For these calculations we assume the sandpaper is 0.5-mm thick, with a density of 0.99 g/cc, a heat capacity of 0.25 cal/g/°C, and a thermal conductivity of 0.028 cal/s/cm/°C. We use PBX 9404 HE shear strengths of 2.0e09 and 2.6e08 dynes/cm², at temperatures of 20 and 331°C, respectively. We calculate that 10-, 6-, and 3-inch diameter hemispheres of PBX 9404 HE dropped on sandpaper targets at a 45 degree incident angle would ignite at minimum drop heights of 1.8, 5.2, and 19.8 feet, respectively. The test data from Table I show that the corresponding 50% drop heights are 4, 5.3 and 23.7 feet, respectively.

If no inert cone or additional mass is attached to the 1-inch diameter hemispheres, we calculate a minimum drop height to ignition of 47 feet. If a 600-g inert cone is attached to the PBX 9404 HE hemisphere, we calculate a minimum drop height of 8 feet. We did not obtain ignition of the 1-inch diameter hemisphere samples in our drop tower tests, even at a drop height of 15 feet. If

the sandpaper target is inclined 30 degrees to the vertical, we calculate a minimum drop height to ignition of 14 feet for the 1-inch diameter hemisphere/inert cone assembly. We have no drop tower or air gun data above 12.1 feet for a target set at a 30 degree incident angle.

The skid impact contact area must be greater than a certain minimum size to provide the inertial and thermal confinement necessary for ignition. Dyer and Taylor² report that a contact area of at least 1 square inch is required to produce a high-order detonation through skid impact. Their experiments with 1/2-inch cubic samples resulted in only partial explosions. Because EXPLO is a one-dimensional code, it cannot account for the change in contact area when different diameter HE samples skid onto flat targets. We need to use a two- or three-dimensional code to model the contact area properly. It is especially important to do this when dealing with small HE samples where the skid impact spot diameter might be less than that required for detonation.

B. DYNA3D Stress Analysis

We did a series of three-dimensional structural analyses using the DYNA3D computer code to quantify the extent of HE breakage with time upon impact loading. DYNA3D is an explicit three-dimensional finite element code for analyzing the large dynamic response of inelastic solids and structures.⁸ The DYNA3D version that we used was written by J. O. Hallquist and R. G. Whirley, LLNL. The three-dimensional meshes were made with the ESCHER and PATRAN codes. ESCHER is an in-house finite element mesh generator written by W. R. Oakes.¹⁰ PATRAN is a pre- and post-processing code written and maintained by PDA Engineering.¹¹ The DYNA3D code generates a binary plot file that can be viewed using TAURUS, an interactive post-processor for the analysis of three-dimensional codes.¹² TAURUS was written by B. E. Brown and J. O. Hallquist, LLNL.

Figure 5 shows our finite element mesh of the projectile assembly before it impacts a 3/8-inch thick x 4-inch wide x 10-inch long aluminum plate set at an incident angle of 45 degrees. The projectile assembly consists of a 1-inch diameter hemisphere of PBX 9404 HE bonded to a 900-10 inert cone, which in turn is attached to a 155-mm diameter steel cylinder. The mesh is made up of 8-node solid hexahedron elements with sliding interfaces between the hemisphere outer surface and the front surface of the plate. We set the

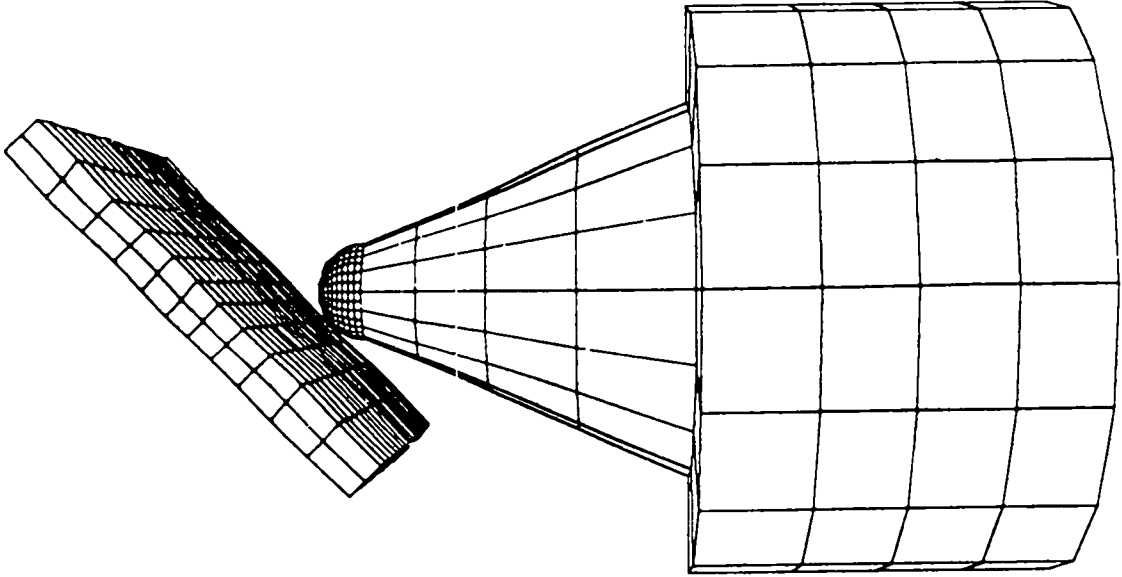


Fig. 5. Finite element mesh of the projectile assembly as it impacts an inclined aluminum plate.

coefficient of friction between these two surfaces to 0.4. We also used fixed interfaces to tie the coarse mesh of the cone to the much finer mesh of the hemisphere.

We used a strain-rate-dependent isotropic plasticity material type for the HE and kinematic hardening elastic-plastic material type for the other materials. The material properties are shown in Table II. In the strain-rate-dependent model, a load curve is used to describe the yield strength, σ_0 , as a function of effective strain rate, $\dot{\bar{\epsilon}}$, where

$$\dot{\bar{\epsilon}} = (2/3\dot{\epsilon}'_{ij}\dot{\epsilon}'_{ij})^{1/2}. \quad (2)$$

The prime denotes the deviatoric component. The yield stress is defined as

$$\sigma_y = \sigma_0(\dot{\bar{\epsilon}}) + E_h\bar{\epsilon}^p, \quad (3)$$

where $\bar{\epsilon}^p$ is the effective plastic strain and E_h is given by

$$E_h = EE_t/(E - E_t). \quad (4)$$

Table 2. Material Properties used in DYNA3D Skid Impact Analysis

Property	PBX 9404	900-10 Inert	Aluminum Alloy	Soft Steel
Density (g/cc)	1.84	1.84	2.7	8.0
Young's Modulus (GPa)	6.8	6.8	70	200
Poisson's Ratio	0.30	0.30	0.33	0.33
Yield Stress (MPa)	*a	62	276	376
Hardening Modulus (MPa)	10	10	700	2000

*For effective strain rates of 0, 3000, and $3.0 \times 10^6 \text{ s}^{-1}$, the yield strength of the HE is 7, 62, and 500 MPa, respectively.

We do not have accurate values for the properties of PBX 9404 HE at extremely high strain rates. This should be taken into account when considering the results of this analysis. Data obtained using our high-speed video system in subsequent tests will be used to improve our material models. These initial analyses are done to compare the effects of using different size samples and slightly different geometries in our tests, and not necessarily to generate an absolute description of the material behavior.

We fixed the outer edges of the plate and set the impact velocity of the projectile assembly to 7.67 m/s. This corresponds to a drop height of 9.9 feet. Figure 6 shows the deformation and maximum principal strain contours in a sequence of selected times after a 1-inch diameter PBX 9404 HE hemisphere impacts an aluminum plate inclined 45 degrees to the initial projectile direction. The figure shows that 0.2 ms after initial contact is made the maximum principal strain exceeds 1%, our chosen failure criteria, in almost half of the sample. Even after 0.35 ms, the maximum diameter of flattened material is less than 1/2-inch. Our drop test data indicate that 1/2-inch is the minimum impact spot diameter required for high-order detonation. Although we continue the analysis until large HE deformations are shown, it is not likely that the specimen will remain intact for 1.05 ms. Figure 7 shows the deformation and maximum principal strain contours in a sequence where a 10-inch diame-

ter PBX 9404 HE hemisphere impacts a steel plate inclined 45 degrees to the initial projectile direction. It takes far longer for the 1% failure strain to travel through the sample. The maximum principal strain exceeds 1% in only a small portion of the specimen even after 1.6 ms. Note the much larger impact contact area with the 10-inch diameter specimen than with the 1-inch diameter sample. Figure 7 shows that the impact spot diameter is more than 1.5 inches, after only 0.35 ms. The large diameter sample test allows more time for the heat generated at the impact area to build to detonation.

Figure 8 shows the deformation and principal strain contours in a sequence where a 1-inch diameter PBX 9404 HE sample impacts an aluminum plate inclined 30 degrees to the initial projectile direction. This sequence shows that it takes almost twice as long for the 1% failure strain to travel through the sample when impacting a target inclined 30 degrees to the initial projectile direction than one inclined 45 degrees. It also shows that the forward end of the inert cone strikes the target about 1 ms after initial contact is made. This decreases the impact force of the HE hemisphere on the target plate. This interference was eliminated by modifying the inert cone to allow us to attach the sample hemisphere to its side rather than its nose.

The finite element mesh of a 1/2-inch high spherical segment of a 3-inch diameter hemisphere attached to the modified projectile assembly is shown in Fig. 9. The figure shows the deformation and principal strain in a time sequence where a PBX 9404 HE sample impacts an aluminum plate inclined 30 degrees to the initial projectile direction at a velocity that corresponds to a drop height of 9.9 feet. We calculate an impact spot diameter of 0.68 inch in 0.35 ms. This sequence shows that it takes longer for the 1% failure strain to travel through the sample, compared to the smaller sample attached to an unmodified projectile assembly.

We used the DYNA3D code to compare the structural behavior of a 3-inch diameter HE hemisphere with a 1/2-inch high spherical segment HE sample attached to the modified projectile assembly. We calculate that dropping a 3-inch diameter PBX 9404 HE hemisphere from 23.4 feet onto a steel target inclined 45 degrees to the vertical produces an impact spot diameter of 0.85 inch. The spherical segment sample impacting an aluminum target plate inclined 30 degrees to the initial projectile direction, at the same velocity, produces an impact spot diameter of 0.75 inch. A comparison of the maximum principal

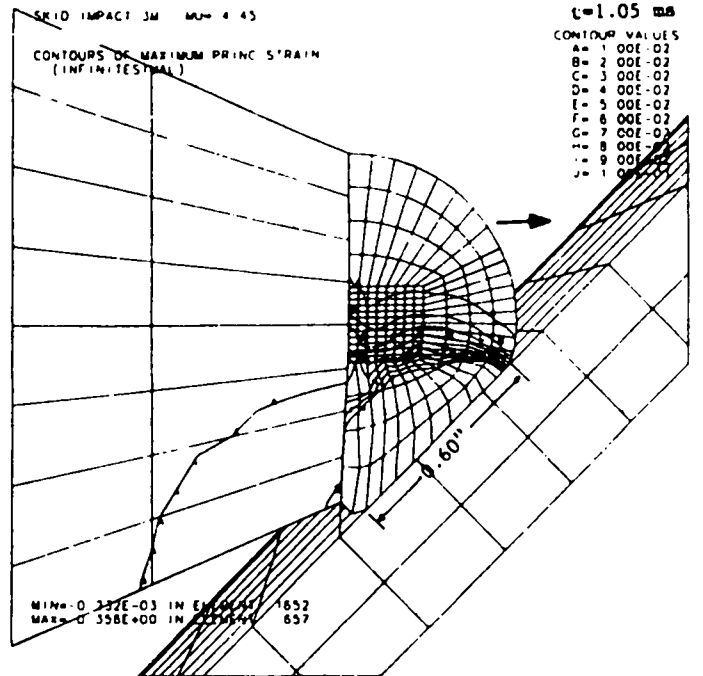
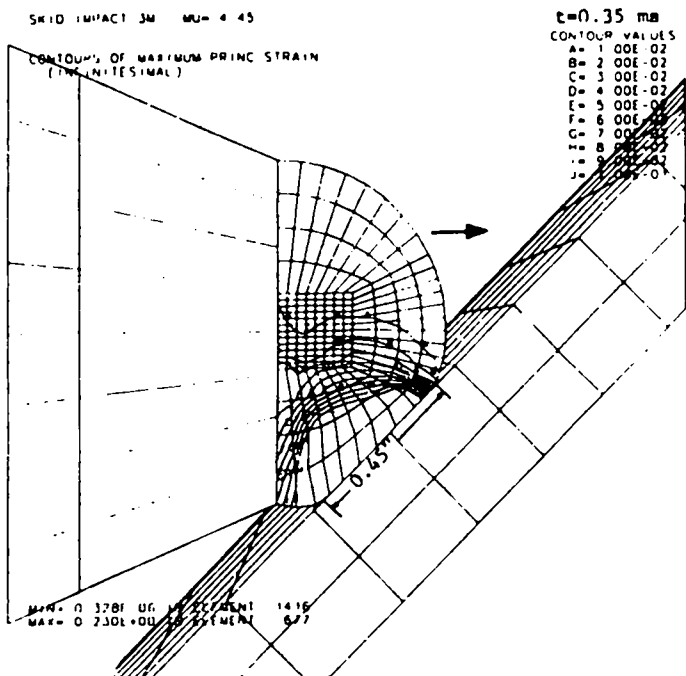
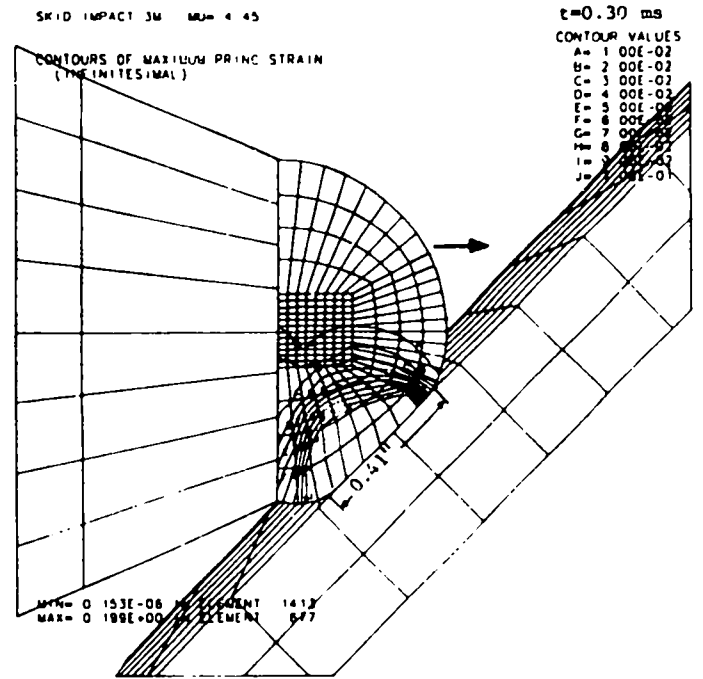
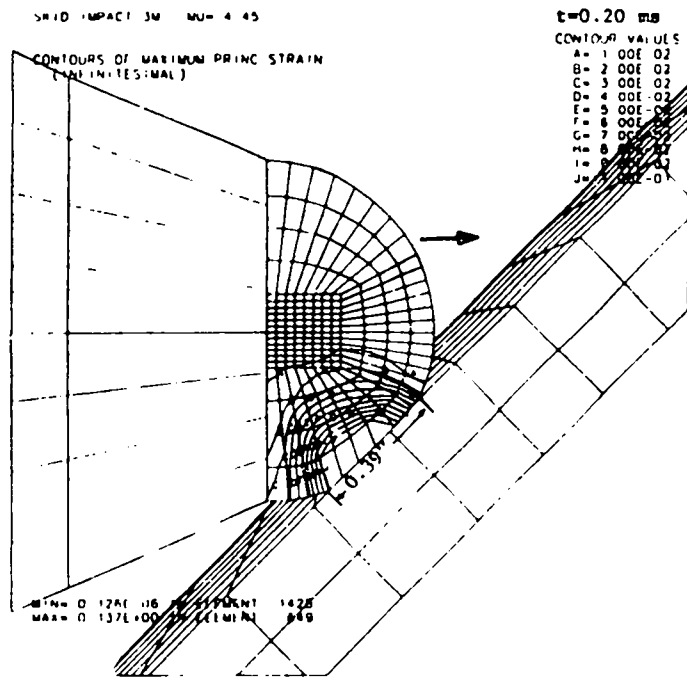


Fig. 6. Deformation and maximum principal strain of 1-inch diameter sample impacting a target plate inclined 45 degrees.

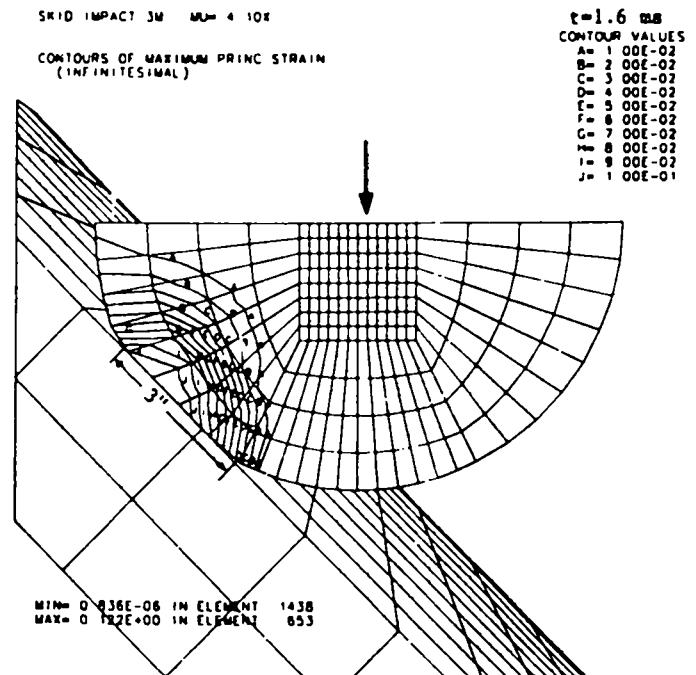
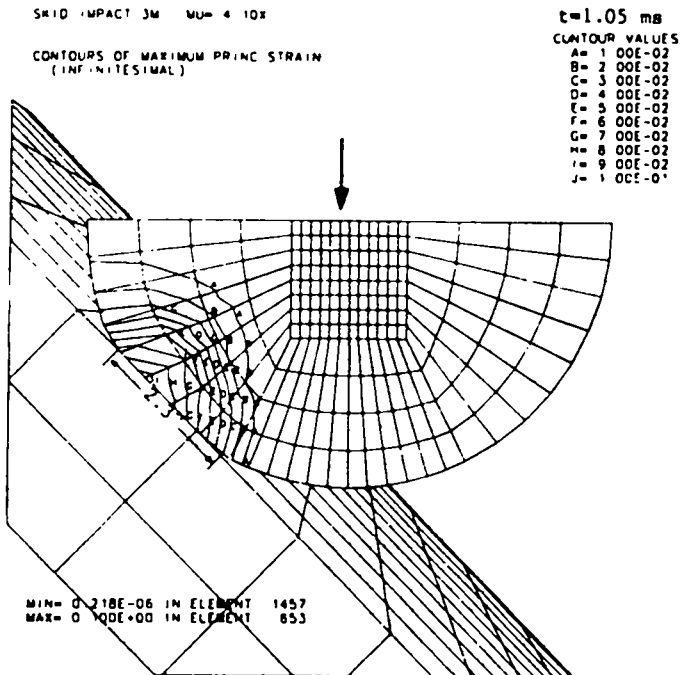
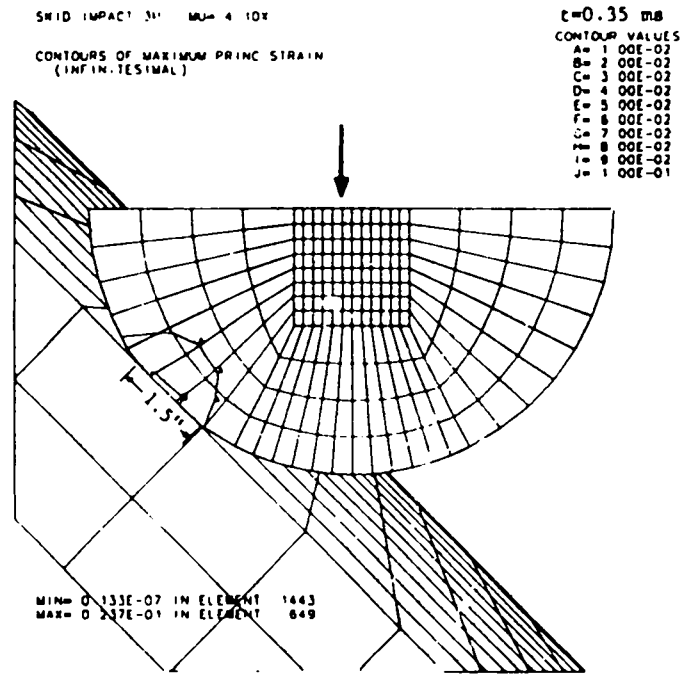
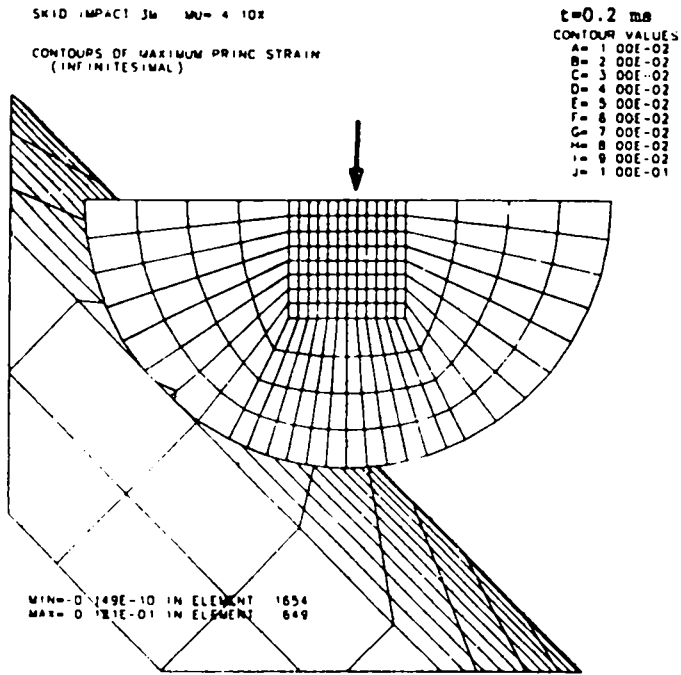


Fig. 7. Deformation and maximum principal strain of 10-inch diameter sample impacting a target plate inclined 45 degrees.

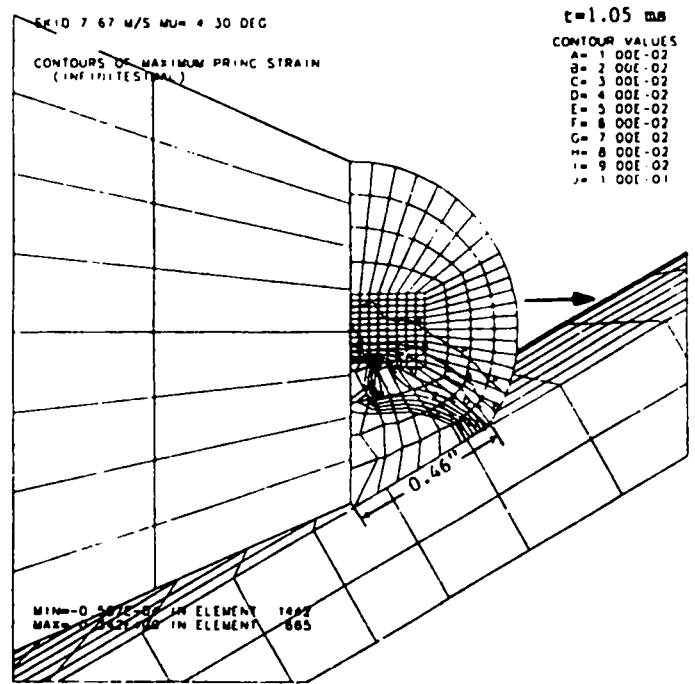
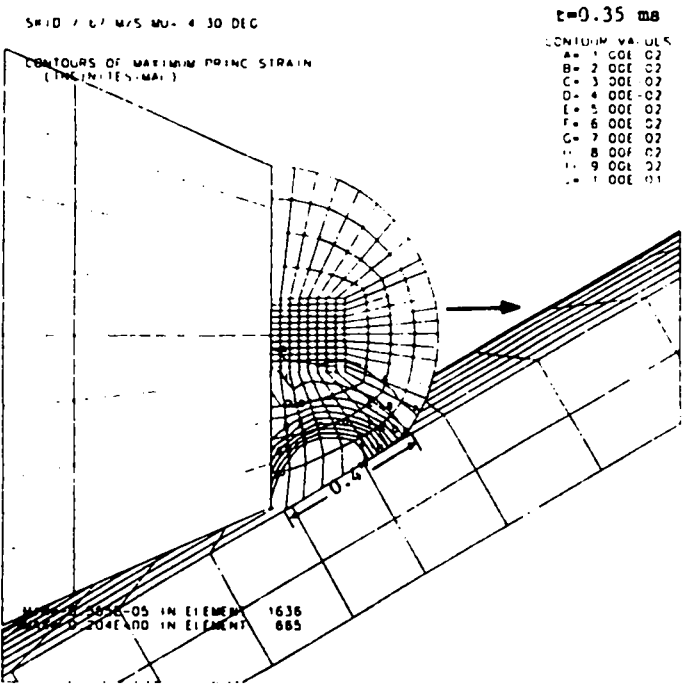
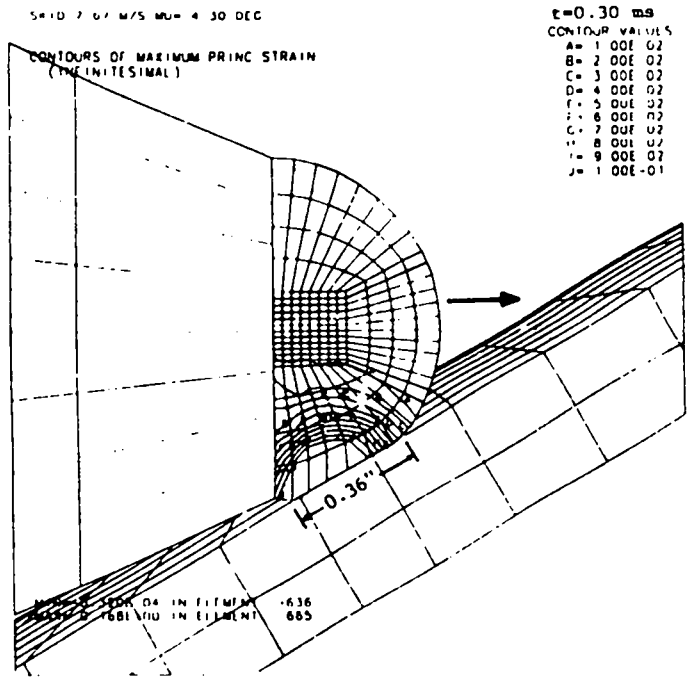
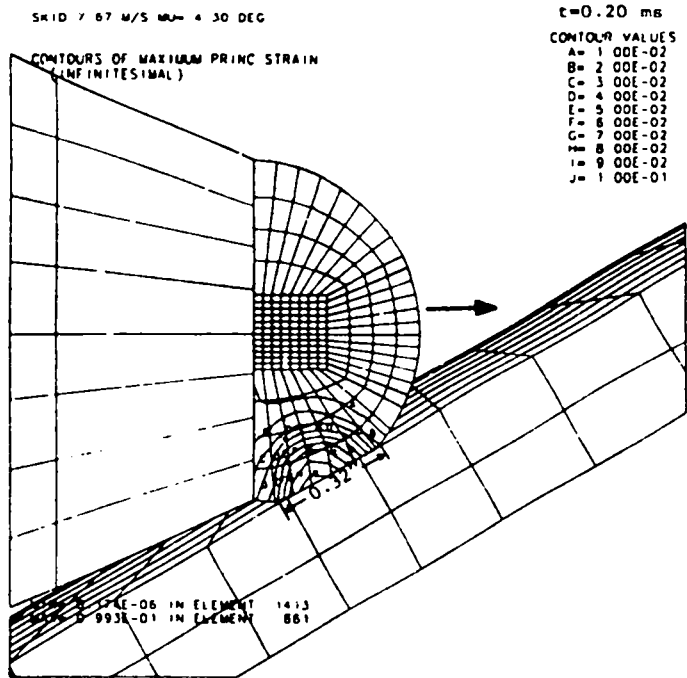


Fig. 8. Deformation and maximum principal strain of 1-inch diameter sample impacting a target plate inclined 30 degrees.

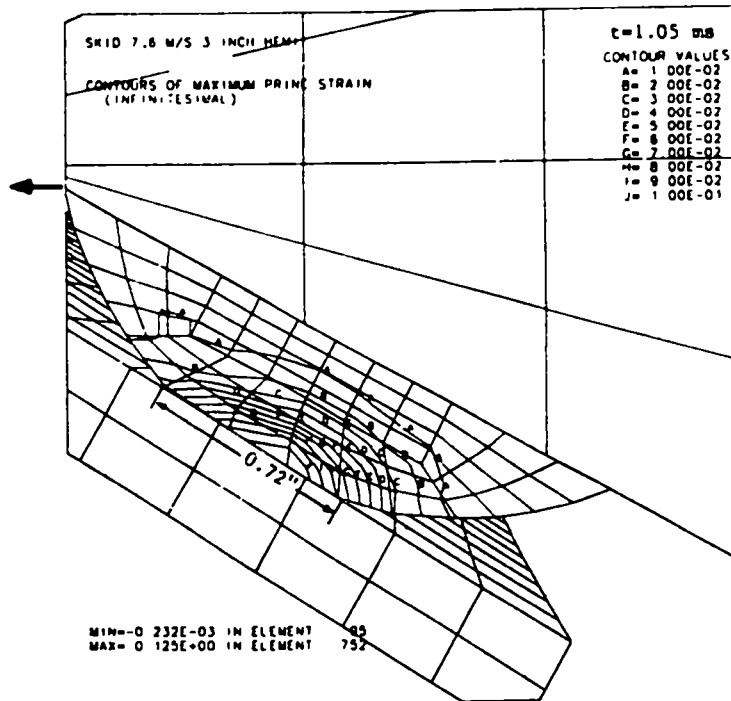
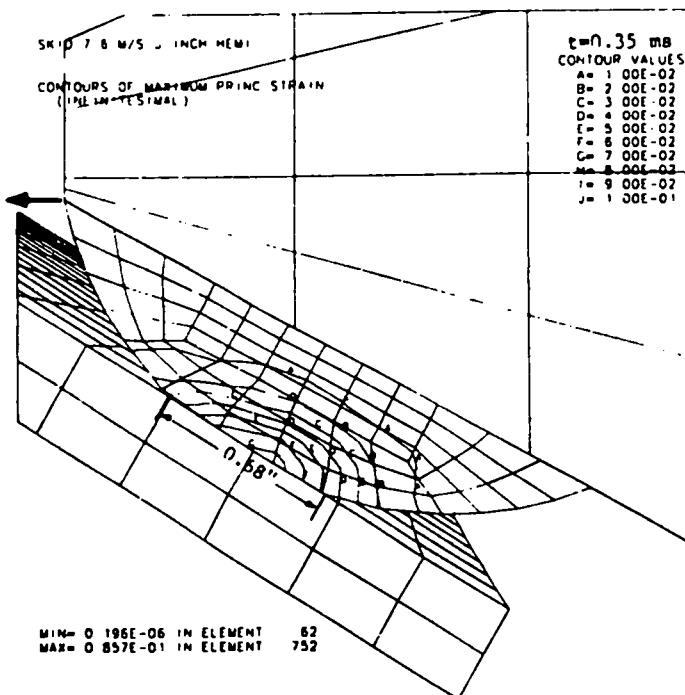
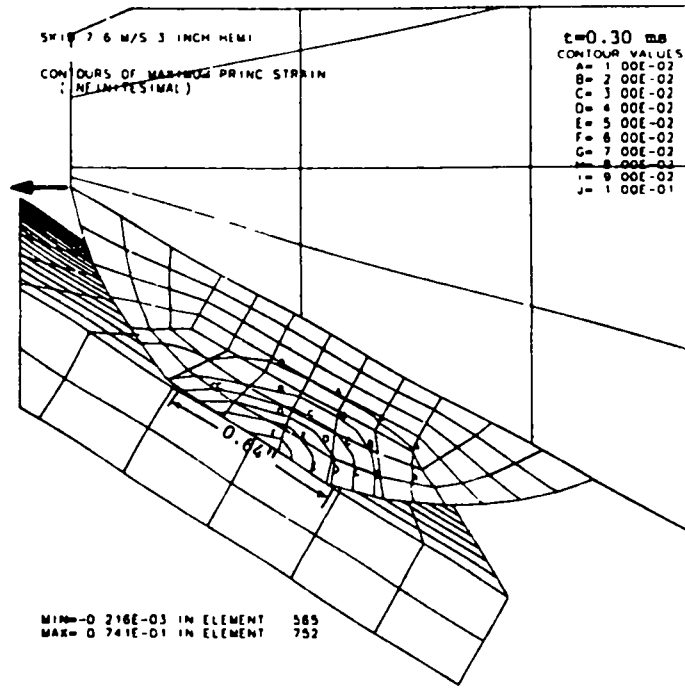
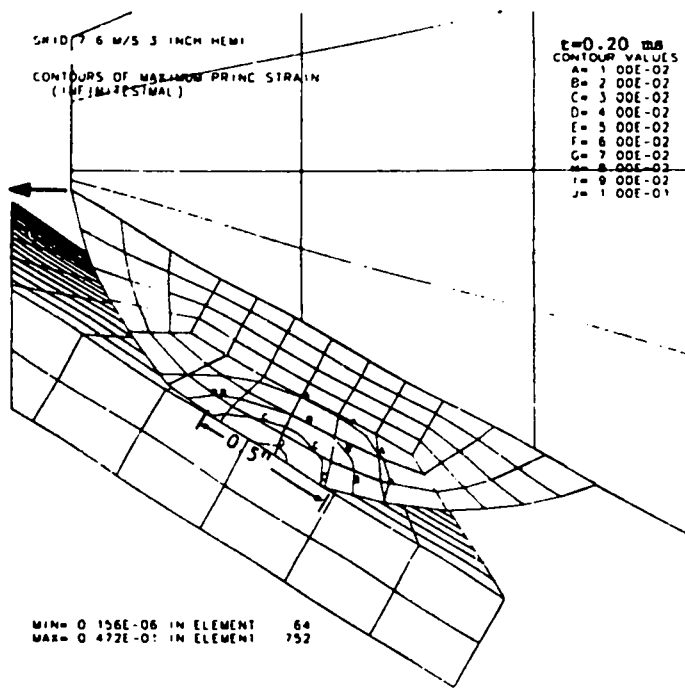


Fig. 9. Deformation and maximum principal strain of 3-inch diameter sample attached to a modified projectile impacting a target plate inclined 30 degrees.

strain contours indicates that the 1% failure strain travels through both test samples in about the same time. Because of our success in detonating the 3-inch diameter hemispheres, we expect to attain high-order detonation of the spherical segment HE samples using the air gun.

C. ABAQUS Heat Transfer and Stress Analysis

We are doing coupled temperature-displacement analyses using the ABAQUS code to study the thermal and structural response of an HE hemisphere impacting a flat target. ABAQUS is a multipurpose finite element code written and maintained by HKS, Inc.⁹ We made the two-dimensional finite element meshes with ESCHER, our in-house mesh generator. Our models are axisymmetric, composed of eight-node quadrilaterals with “rigid surfaces” and “slide lines” at the appropriate interfaces. Because of the integration procedure used in ABAQUS transient heat transfer, HKS suggests that the minimum usable time step should be directly proportional to the square of a typical element dimension.⁹ If too small a time step is used, spurious oscillations can appear in the solution. Because HE ignition by skid impact occurs in less than 0.50 ms,² we need to use time steps as small as 10 microseconds. This limits the size of the elements in our mesh to less than 0.00026 mm. Hundreds of thousands of elements of this size are required to model a square inch of contact area.

Our ABAQUS models have evolved from coarse, finite element meshes of the complete projectile assembly and target plate, similar to that shown in Fig. 5, to much finer meshes that model only the immediate region of the impact area. We are searching for a way to bypass this algorithm to determine the solution of a 3-inch diameter sample impacting a target at a 30 degree incident angle.

V. SUMMARY AND CONCLUSIONS

Our computer analysis indicates that we can increase the time required for the failure strain to travel through small HE samples by impact testing at incident angles less than 45 degrees. We can increase the impact spot diameter past the minimum size required for high-order detonation by increasing the diameter of our test samples. We have modified our air gun projectile assembly to allow testing with these parameters and to permit clean sample-target impact at shallow incident angles.

We have not obtained a full-scale detonation of a high explosive sample that is small enough to be tested in close proximity to our infrared equipment. However, we are confident that we can consistently obtain detonation in our skid impact tests by using the optimum conditions for the ignition of small HE samples. These optimum conditions include: 1) testing samples of PBX 9404 HE, the most sensitive, commonly-used secondary high explosive at Los Alamos, 2) testing 1/2-inch high spherical segments of 3-inch diameter samples that are large enough to provide sufficient thermal and inertial confinement at impact, 3) using targets of salt or sapphire, inclined 30 degrees to the initial projectile direction, 4) using either targets with roughened surfaces or gluing grit particles to smooth target surfaces to provide nucleation sites for ignition hot spots and increase heat generation through friction, and 5) testing the samples at impact velocities greater than that corresponding to a drop height of 23.7 feet, the 50% drop height of 3-inch diameter PBX 9404 HE.

We have acquired the equipment and developed the methods needed to measure the transient heating produced in the ignition of an explosive sample as it impacts an IR transmissive target. We will resume testing inert and high explosive samples when cost and schedule constraints permit.

REFERENCES

1. W. G. Von Holle, "Temperature Measurement of Shock Heated Solid Explosives by Time Resolved Infrared Radiometry," Symposium H.D.P. Comportement des Milieux Denses Sous Hautes Pressions Dynamiques, Paris, France (October 1978).
2. A. S. Dyer and J. W. Taylor, "Initiation of Detonation by Friction on a High Explosive Charge," The Fifth Symposium on Detonation, Pasadena, CA (August 1970).
3. A. D. Randolph, L. E. Hatler, and A. Popolato, "Rapid Heating-to-Ignition of High Explosives. I. Friction Heating," I and EC Fundamentals, Vol. 15, p. 1 (February 1976).
4. T. Gibbs and A. Popolato, eds., "LASL Explosives Property Data," Berkeley: University of California Press (1980).
5. B. M. Dobratz and P. C. Crawford, "LLNL Explosives Handbook Properties of Chemical Explosives and Explosive Simulants," Lawrence Livermore National Laboratory, UCRL-52997, Change 2 (January 1985).
6. W. J. Dixon and F. J. Massey, "Introduction to Statistical Analysis," pp. 319-327, McGraw-Hill, New York, NY (1957).
7. D. L. Jaeger and A. S. Vigil, "EXPLO: Explosives Thermal Analysis Computer Code," Los Alamos National Laboratory report LA-6949-MS, Rev. 2 (October 1987).
8. J. O. Hallquist and R. G. Whirley, "DYNA3D User's Manual (Nonlinear Dynamic Analysis of Structures in Three Dimensions)," Lawrence Livermore National Laboratory report UCID-19592, Rev. 5 (May 1989).
9. Hibbet, Karlsson and Sorensen, Inc., "ABAQUS User's Manual, Vers. 4-7," 100 Medway Street, Providence, RI (1988).
10. W. R. Oakes, Jr., "Learning to Use the Finite-Element Mesh Generator, ESCHER 3.2," Los Alamos National Laboratory report LA-11448-MS, UC-706 (August 1989).
11. PDA Engineering Software Products Division, "PATRAN II User's Guide," 1560 Brookhollow Drive, Santa Ana, CA (1986).
12. B. E. Brown and J. O. Hallquist, "TAURUS: An Interactive Post-Processor for the Analysis Codes NIKE3D, DYNA3D, TACO3D, and GEMINI," Lawrence Livermore National Laboratory report UCID-19392, Rev. 1 (May 1984).